

# Visualization of the projective line geometry for geometric algebra

---

Drawing lines in GAViewer

Patrick M. de Kok  
5640318

Bachelor thesis  
Credits: 18EC

Bacheloropleiding Kunstmatige Intelligentie

University of Amsterdam  
Faculty of Science  
Science Park 904  
1098 XH Amsterdam

*Supervisor*

Dr.ir. Leo Dorst

Intelligent Systems Laboratory Amsterdam  
Faculty of Science  
Science Park 904  
1098 XH Amsterdam

July 24th, 2012

## Abstract

This thesis describes a method for computationally recognizing the geometrical interpretation of most blades of the model of projective line geometry in geometric algebra. These different interpretations are not merely recognizable by the grade of the elements, or the absence or presence of some basis vector, as can be done for the homogeneous model for geometric algebra. GAViewer, a graphical calculator for the Euclidean and conformal models of geometric algebra, is extended to implement the projective line geometry and its visualization.

**Keywords:** Geometric algebra, projective geometry, Plücker coordinates, homogeneous representation.

# Contents

<b>1</b>	<b>Introduction</b>	<b>1</b>
1.1	Project aim and document structure . . . . .	2
<b>2</b>	<b>Line geometry and geometric algebra</b>	<b>3</b>
2.1	Geometric algebra . . . . .	3
2.2	Plücker model . . . . .	5
2.2.1	Intersecting lines . . . . .	9
<b>3</b>	<b>Classifying and parameterizing elements of different geometric interpretations</b>	<b>11</b>
3.1	Blades of grade 0 and 6 . . . . .	11
3.2	Blades of grade 1 and 5 . . . . .	11
3.3	Blades of grade 2 and 4 . . . . .	12
3.4	Blades of grade 3 . . . . .	14
<b>4</b>	<b>Implementation</b>	<b>17</b>
4.1	Software design decision . . . . .	17
4.2	Computing with 13ga in GAViewer . . . . .	18
4.3	Models and casting . . . . .	18
4.4	Blade interpretation and visualization . . . . .	19
4.4.1	Grade 0 . . . . .	20
4.4.2	Grade 1 . . . . .	20
4.4.3	Grade 2 . . . . .	21
4.4.4	Grade 3 . . . . .	22
4.4.5	Grade 4 . . . . .	23
4.4.6	Grade 5 . . . . .	23
4.4.7	Grade 6 . . . . .	23
4.5	User interaction . . . . .	23
<b>5</b>	<b>Conclusion</b>	<b>25</b>
<b>A</b>	<b>Visualizations</b>	<b>27</b>
	<b>Bibliography</b>	<b>39</b>

# 1 Introduction

Just as linear algebra, geometric algebra is an algebra over a given vector space  $\mathbb{R}^n$ . The difference lies in its operations; whereas linear algebra relies on matrix manipulations, geometric algebra's base operation is the geometric product. From this product, one can deduce the inner product, known from linear algebra, and the outer product. The outer product of two vectors  $\mathbf{a}$  and  $\mathbf{b}$  represents the set of elements that are linear combinations of its operands  $\{\alpha\mathbf{a} + \beta\mathbf{b} \mid \alpha, \beta \in \mathbb{R}\}$ .

There are several models of geometry in use in the geometric algebra community, of which the conformal model is the most popular and widely known [4]. Although its angle-preserving transformations are usable in many cases, some problems need to be tackled by projective transformations. These transformations are an important class of operations within computer vision and computer graphics.

GAViewer is a visualization and computing tool for the 3-dimensional Euclidean, homogeneous and conformal models of geometric algebra, developed by Daniel Fontijne at the University of Amsterdam [5]. It allows the user to perform calculations in selected models of geometric algebra, and shows the results, both numerically and graphically. Moreover, it allows the user to rotate, translate and zoom the viewport, as well as to manipulate the displayed elements. The variables in which they are stored are automatically updated, and, if desired by the user, other objects that are parameterized by the manipulated object may be updated dynamically as well.

Recently, Li and Zhang [7] have found a way to model projective geometry, using a 6 dimensional representation space  $\mathbb{R}^{3,3}$  with a special metric structure, which allows three of its basis vectors to square to  $-1$ . Using Plücker coordinates [4, 7, 8, 9], weighted lines are represented in the representation space by vectors  $v$  satisfying the Plücker condition  $\Omega_q(v) = v^2 = vv = v \cdot v = 0$ . As a consequence, there are also vectors  $w$  in the representation space with  $w^2 \neq 0$  which do not represent lines. Objects with different geometrical interpretations are generated by the outer product over lines and non-lines. For example, for two intersecting lines  $a$  and  $b$ , the outer product represents a pencil of lines; the set of all lines that are in the same plane as  $a$  and  $b$ , and pass through the same point. The outer product of two skew lines  $a'$  and  $b'$  is interpreted as the set of those two lines.

In their article, Li and Zhang have not discussed what each element in their algebra might represent. Barrau [2, 1] and Pottmann and Wallner [8, Chapter 2 and 3] have investigated the objects that can be represented in a 6-dimensional space with Plücker coordinates, both using different algebras from ours. Pottmann and Wallner use linear algebra and Grassmann algebra, while Barrau's algebra has less expressive power.

## 1.1 Project aim and document structure

GAViewer is a multi-purpose program for performing geometric algebra computations and visualizing geometric algebra [5]. The aim of this project is to augment GAViewer so it can interpret the Plücker model for geometric algebra. Besides knowing how to evaluate textual expressions to objects of the algebra, GAViewer needs new interpretation and visualization algorithms. For this, we show the relation between many blades of the model presented by Li and Zhang [7] and the elements described by Pottmann and Wallner [8].

In section 2, a brief introduction to geometric algebra and the Plücker model for linear algebra are given. The algebra and model are coupled by interpreting the inner product with the help of the homogeneous model. Section 3 demonstrates the geometric interpretation of several blades of the Plücker model. The computation of characteristics needed to draw certain blades together with their sensible visualization are described in section 4. A rendering of a representative of each class of geometrically different objects is presented in appendix A.

Section 5 presents the reader a summary of the results of this thesis, together with a discussion of this work as well as possible future work. The document concludes with a bibliography.

## 2 Line geometry and geometric algebra

Geometric algebra is a mathematical framework for expressing geometric problems in a structure-preserving way. This means that, in a well-defined model, applying an operation on a composed object of the algebra results in the same object as when one decomposes the object, applying the same operation on its decomposition, and compose the new object from the transformed elements. Models that have this property, are called operational.

The system of Plücker coordinates is another framework for geometric problems; more specifically, projective line geometry. It is often used with linear algebra and computer graphics [9], and there have been non-operational models based on the homogeneous model in geometric algebra [4, Chapter 12]. Recently, an operational model has been designed [7].

Subsection 2.1 presents a short, incomplete introduction to geometric algebra, while the operational model of Plücker coordinates for geometric algebra is explained in subsection 2.2. For a more in-depth and complete discussion of geometric algebra, we refer to Dorst et al. [4].

### 2.1 Geometric algebra

This section presents a selection of material from Chapters 2 through 7, and 11 from Dorst et al. [4], which explains the operations of the algebra used in this thesis. Vectors values are notated with lower-case Latin letters. We often use symbols from the Greek alphabet to indicate a variable has a scalar value, or use lower-case Latin letters where they are traditionally used and cannot be confused with vectors. Euclidean elements of the algebra are written with a bold font. All variables not representing scalar or vector values are printed with a capital letter.

Both linear algebra and geometric algebra are defined over an  $n$ -dimensional vector space  $\mathbb{R}^n$ . A well-known example of such a vector space is  $\mathbb{R}^3$ , the Euclidean vector space, where each vector represents a direction. We choose an arbitrary orthonormal basis  $\{\mathbf{e}_1, \mathbf{e}_2, \mathbf{e}_3\}$ . The homogeneous space  $\mathbb{R}^4$  add a fourth basis vector  $e_0$  to compute with. This element is interpreted as a point at an arbitrarily chosen origin. Addition of a direction  $\mathbf{d}$  to a point  $p = \mathbf{p} + e_0$  results in a point at location  $\mathbf{d} + \mathbf{p}$ . When  $p$  is composed of a multiple  $\lambda$  of the origin  $e_0$ , we say it has weight  $\lambda$ , and is at location  $\mathbf{p}/\lambda$ .

Both algebras define an inner product on two vectors  $v, w$  from the space  $\mathbb{R}^n$ . The inner product of two vectors  $v \cdot w$  results in a scalar, and gives both algebras access to the range of real numbers  $\mathbb{R}$ . The inner product can be defined in terms of the matrix product. Let us define a metric and represent it by its matrix  $\llbracket M \rrbracket$  for the Euclidean space. Given its basis, let  $\mathbf{v} = \lambda_1 \mathbf{e}_1 + \lambda_2 \mathbf{e}_2 + \lambda_3 \mathbf{e}_3$  and  $\mathbf{w} = \mu_1 \mathbf{e}_1 + \mu_2 \mathbf{e}_2 + \mu_3 \mathbf{e}_3$  correspond with  $\llbracket \mathbf{v} \rrbracket = \llbracket \lambda_1, \lambda_2, \lambda_3 \rrbracket^\top$  and  $\llbracket \mathbf{w} \rrbracket = \llbracket \mu_1, \mu_2, \mu_3 \rrbracket^\top$ . The inner product can be

defined as follows:

$$\begin{aligned}
\mathbf{v} \cdot \mathbf{w} &= \llbracket \mathbf{v} \rrbracket^T \llbracket M \rrbracket \llbracket \mathbf{w} \rrbracket \\
&= \llbracket \mathbf{v} \rrbracket^T \begin{bmatrix} \mathbf{e}_1 \mathbf{e}_1 & \mathbf{e}_1 \mathbf{e}_2 & \mathbf{e}_1 \mathbf{e}_3 \\ \mathbf{e}_2 \mathbf{e}_1 & \mathbf{e}_2 \mathbf{e}_2 & \mathbf{e}_2 \mathbf{e}_3 \\ \mathbf{e}_3 \mathbf{e}_1 & \mathbf{e}_3 \mathbf{e}_2 & \mathbf{e}_3 \mathbf{e}_3 \end{bmatrix} \llbracket \mathbf{w} \rrbracket \\
&= \llbracket \mathbf{v} \rrbracket^T \begin{bmatrix} 1 & 0 & 0 \\ 0 & 1 & 0 \\ 0 & 0 & 1 \end{bmatrix} \llbracket \mathbf{w} \rrbracket \\
&= \begin{bmatrix} \lambda_1 & 0 & 0 \\ 0 & \lambda_2 & 0 \\ 0 & 0 & \lambda_3 \end{bmatrix} \llbracket \mathbf{w} \rrbracket \\
&= \lambda_1 \mu_1 + \lambda_2 \mu_2 + \lambda_3 \mu_3.
\end{aligned}$$

In this case, the metric matrix is the identity matrix. For other spaces, we might have to define different metric matrices. We say that an algebra is in metric space  $\mathbb{R}^{p,q}$  if the metric matrix  $M$  can be written as a diagonal matrix with  $p$  occurrences of 1 and  $q$  occurrences of  $-1$  for at least one of the bases of  $\mathbb{R}^{p+q}$ .

But from here the ways part for linear algebra and geometric algebra. Linear algebra knows only vectors and scalars as objects, while matrices correspond to linear maps. Geometric algebra defines a multivector space  $\bigwedge \mathbb{R}^n$  through its outer product. For two vectors  $a$  and  $b$ , their outer product, or wedge product, is denoted by  $a \wedge b$ . The product spans the subspace of  $a$  and  $b$ ; the wedge product represents the set of elements that are linear combinations of its constituents. When  $a$  can be expressed as a linear combination of  $b$ , the product results in zero. The outer product can be applied to any object of the algebra, generating a  $\sum_{0 \leq i \leq n} \binom{n}{i} = 2^n$  dimensional multivector basis for  $\mathbb{R}^n$ . Multivector spaces generalize the concept of a vector space, and a multivector space generated by a vector space  $\mathbb{R}^n$  is denoted by  $\bigwedge \mathbb{R}^n$ . When a multivector consists of elements of the same dimensionality  $k$  (every basis element can be made by the same number of outer product applications), we say it is of grade  $k$ , and call its multivector a  $k$ -vector. By this definition, vectors and scalars are 1 and 0-vectors, respectively. The highest-grade element of the space is called the pseudoscalar  $I_{p,q}$ . When a  $k$ -vector can be written as the outer product of vectors, it is called a  $k$ -blade. The set of  $k$ -vectors is notated by  $\bigwedge^k \mathbb{R}^n$ . A noteworthy property of the outer product is its antisymmetry. The blade  $A \wedge B$  equals  $-B \wedge A$ . Reversing the order in which the outer product is applied to get a blade  $A = a_1 \wedge a_2 \wedge \cdots \wedge a_{k-1} \wedge a_k$  to  $a_k \wedge a_{k-1} \wedge \cdots \wedge a_2 \wedge a_1 = (-1)^{x(x-1)/2}$  happens so often, it has its own shorthand notation  $\tilde{A}$ .

With these new elements, we have to extend the definition of the inner product, so it can be applied to  $(k > 1)$ -vectors. This gives rise to the contraction, written  $A \rfloor B$  for  $a$ -vector  $A$  and  $b$ -vector  $B$ . Dorst et al. summarize

the geometrical interpretation of the contraction by stating: “The contraction  $\mathbf{A}$  on  $\mathbf{B}$  of an  $a$ -blade  $\mathbf{A}$  and a  $b$ -blade  $\mathbf{B}$  is a specific subblade of  $\mathbf{B}$  of grade  $b - a$  perpendicular to  $\mathbf{A}$ , with a weight proportional to the norm of  $\mathbf{B}$  and to the norm of the projection of  $\mathbf{A}$  onto  $\mathbf{B}$ ” [4, p.76]. This corresponds with the dot product for vectors: the contraction produces a 0-blade. When  $a > b$ , the grade is negative. Because there are no negative-grade elements defined for our algebra, the contraction evaluates to 0.

Note that 0 is treated as an element of a negative grade. In our multivector space, there is no need to make a distinction between zero blades of different grades; all will be notated with 0, and 0 is treated as having any grade.

Both these products can be defined in terms of the geometric product. For vectors  $a$  and  $b$ , it defines the inner and outer product as  $a \rfloor b = a \cdot b = \frac{1}{2}(a \cdot b + b \cdot a)$  and  $a \wedge b = \frac{1}{2}(a \cdot b - b \cdot a)$ . It is an invertible product, and we denote the inverse of a blade  $A$  by  $A^{-1}$ .

A common operation of geometric algebra is taking the orthogonal complement of a  $k$ -blade  $A_k$  with respect to the pseudoscalar. The resulting blade  $A_k^*$  is called the dual of  $A_k$ , and can be computed as  $A_k^* = A_k \rfloor I_{p,q}^{-1} = A_k \rfloor (-1)^q I_{p,q}^{-1}$ . Note that  $A_k = (A_k^*)^*$  does not hold in the general case; if  $q$  and  $p + q$  are not both even, the sign is flipped. Therefore we define a undualization operator:  $A_k = (A_k^*)^{-*}$ .

By taking the dual, we can redefine the cross product of two vectors  $\mathbf{a}$  and  $\mathbf{b}$  from the Euclidean space  $\mathbb{R}^3$ . The cross product  $\mathbf{a} \times \mathbf{b}$  is defined to give the vector orthogonal and proportional to  $\mathbf{a}$  and  $\mathbf{b}$ . If it is orthogonal to these two vectors, it must be orthogonal to all their linear combinations as well. In other words, we want the vector that is proportional and orthogonal to the outer product of  $\mathbf{a}$  and  $\mathbf{b}$ . This is expressed as  $(\mathbf{a} \wedge \mathbf{b}) \rfloor \mathbf{I}_3^{-1}$ .

## 2.2 Plücker model

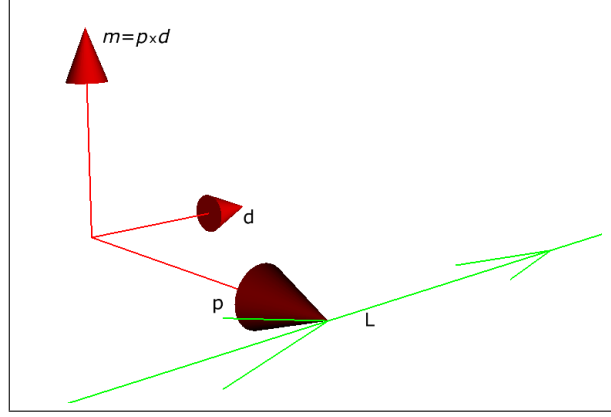
We summarize terms and notations of the Plücker model as treated in Chapter 12 of Dorst et al. [4].

Weighted, infinitely-extending lines of  $\mathbb{R}^3$  have 5 degrees of freedom. Such a line  $L$  can be fully described by five numerical quantities. A common representation follows. As the first three quantities, we take the weighted direction, given by a vector  $\mathbf{d} \in \mathbb{R}^3$ . The weight is encoded as the norm of  $\mathbf{d}$ :  $w(L) = \|\mathbf{d}\|$ . This implies that the unit direction is given by  $\mathbf{d} / \|\mathbf{d}\|$ . We also need to know its displacement from the origin. This will be given by a vector  $\mathbf{p} \in \mathbb{R}^3$ , directed at a point on  $L$ . The point should be chosen so that  $\mathbf{p}$  is orthogonal to  $\mathbf{d}$ . With this fact, we have limited the degrees of freedom of these 6 parameters to 5. These vectors are denoted in figure 1.

In the homogeneous model, the line through weighted points  $p = \lambda_p(e_0 +$



**Figure 1:** A weighted line  $L$  can be defined by any two of its weighted direction  $\mathbf{d}$ , a vector  $\mathbf{p}$  orthogonal to the line, and its moment  $\mathbf{m} = \mathbf{p} \times \mathbf{d}$ .



$\mathbf{p}$ ) and  $q = \lambda_q(e_0 + \mathbf{q})$  with weight  $\lambda_p\lambda_q$  is represented as

$$\begin{aligned} L &= p \wedge q \\ &= (\lambda_p e_0) \wedge (\lambda_q \mathbf{q}) + (\lambda_p \mathbf{p}) \wedge (\lambda_q e_0) + (\lambda_p \mathbf{p}) \wedge (\lambda_q \mathbf{q}) \\ &= \lambda_p \lambda_q (e_0 \wedge (\mathbf{q} - \mathbf{p}) + \mathbf{p} \wedge \mathbf{q}), \end{aligned}$$

with the following dependency relationship:

$$\Omega_q(L) = \lambda_p \lambda_q (e_0 \wedge (\mathbf{q} - \mathbf{p}) \wedge (\mathbf{p} \wedge \mathbf{q})) = 0. \quad (1)$$

Through this relation, the 8 parameters of this representation (3 for  $\mathbf{p}$ , 3 for  $\mathbf{q}$ , 1 for  $\lambda_p$  and 1 for  $\lambda_q$ ) have only 5 degrees of freedom.

The classical parameters to characterize a line, its direction and moment, are easily recognized in this expression. The direction  $\mathbf{d} = \mathbf{p} - \mathbf{q}$  is encoded in the first factor as  $e_0 \wedge -\mathbf{d} = \mathbf{d} \wedge e_0 = \mathbf{d}e_0$ . The moment  $\mathbf{m} = \mathbf{p} \times \mathbf{q} = (\mathbf{p} \wedge \mathbf{q}) \rfloor \mathbf{I}_3^{-1}$  can be found in the second term as  $\mathbf{m} \rfloor \mathbf{I}_3 = ((\mathbf{p} \wedge \mathbf{q}) \rfloor \mathbf{I}_3^{-1}) \rfloor \mathbf{I}_3 = \mathbf{p} \wedge \mathbf{q}$ , which results in another general formula for lines:

$$L = \mathbf{d}e_0 + \mathbf{m} \rfloor \mathbf{I}_3.$$

Within classical literature of linear algebra, the same object is written as  $-\{\mathbf{d} : \mathbf{m}\}$ , using Plücker coordinates to denote a line as a 6D vector. The constraint of equation 1 is expressed as

$$\Omega_q(L) = \mathbf{d} \cdot \mathbf{m} = 0. \quad (2)$$

The relation from equation 1 and equation 2 are indeed equal:

$$\begin{aligned}
e_0 \wedge (\mathbf{q} - \mathbf{p}) \wedge (\mathbf{p} \wedge \mathbf{q}) &= e_0 \wedge \mathbf{d} \wedge (\mathbf{m} \rfloor \mathbf{I}_3) \\
&= \mathbf{d} \wedge (\mathbf{m} \rfloor \mathbf{I}_3) \\
&= \mathbf{d} \cdot (\mathbf{m} \rfloor \mathbf{I}_3) \rfloor \mathbf{I}_3^{-1} \\
&= \mathbf{d} \cdot \mathbf{m}.
\end{aligned}$$

Pottmann and Wallner show this as well [8, Lemma 2.1.2], and name this relationship the Plücker identity. Based on this identity, a bilinear form is defined as:  $\Omega(L_1, L_2) = \Omega_q(L_1 + L_2) - \Omega_q(L_1) - \Omega_q(L_2)$ . Note that when  $L_1 = L_2$ , we have  $\Omega(L_1, L_2) = 2\Omega_q(L_1) = 2\Omega_q(L_2)$ .

The set of 6D vectors  $\{-\{\mathbf{d} : \mathbf{m}\}\}$  that comply with this constraint corresponds to the points on the Klein quadric.

The Plücker coordinates of a line are often treated as just six slots for storing numbers. In most cases, operations on these elements are defined to manipulate two 3D vectors,  $\mathbf{d}$  and  $\mathbf{m}$ , instead of the whole 6D element.

Because of this, the user is often unaware of most of the algebraic structure. In fact, this 6D vector corresponds to

$$L = d_1 e_0 \mathbf{e}_1 + d_2 e_0 \mathbf{e}_2 + d_3 e_0 \mathbf{e}_3 + m_1 \mathbf{e}_2 \mathbf{e}_3 + m_2 \mathbf{e}_3 \mathbf{e}_1 + m_3 \mathbf{e}_1 \mathbf{e}_2.$$

The set  $\{e_0 \mathbf{e}_1, e_0 \mathbf{e}_2, e_0 \mathbf{e}_3, \mathbf{e}_2 \mathbf{e}_3, \mathbf{e}_3 \mathbf{e}_1, \mathbf{e}_1 \mathbf{e}_2\}$  forms an orthogonal and complete basis of the bivectors of the homogeneous model of  $\mathbb{R}^3$  with inner product  $e_0^2 = \mathbf{e}_1^2 = \mathbf{e}_2^2 = \mathbf{e}_3^2 = 1^1$ . The basis is orthogonal, because for any two elements  $E_1, E_2$  it holds that  $E_1 \rfloor E_2 = 0$ . It is also complete; it contains  $\binom{4}{2} = 6$  linear independent elements.

The Plücker model uses these six elements as its basis; it treats these bivectors as 1-dimensional elements. These elements will be known as  $\{e_{01}, e_{02}, e_{03}, e_{23}, e_{31}, e_{12}\}$ . Li and Zhang [7] define an embedding from the Plücker model to the homogeneous model:<sup>2</sup>

$$\text{Em}(A) = \begin{cases} e_0 \wedge \mathbf{e}_i & \text{if } A = e_{0i}; \\ \mathbf{e}_i \wedge \mathbf{e}_j & \text{if } A = e_{ij}; \\ \text{Em}(B) + \text{Em}(C) & \text{if } A = B + C; \\ \text{Em}(B) \wedge \text{Em}(C) & \text{if } A = B \wedge C; \\ [\text{Em}(B) \wedge \text{Em}(C)] & \text{if } A = B \rfloor C. \end{cases} \quad (3)$$

In the last line, the inner product for the Plücker model is defined. The bracket returns the proportionality factor of  $\text{Em}(y) \wedge \text{Em}(z)$  to the homogeneous pseudoscalar  $e_0 \mathbf{I}_3$ . Giving the homogeneous space metric structure

<sup>1</sup>The homogeneous model does not have a natural metric. Some sources choose for  $e_0^2 = -1$ , while others work with  $e_0^2 = 1$ . Its inverse depends on this definition;  $e_0^{-1} = -e_0$  if  $e_0^2 = -1$ . With our chosen metric,  $e_0^{-1} = e_0$ .

<sup>2</sup>This definition of the embedding function  $\text{Em}$  is not the same as the one given by the internal report [3]. The internal report defines its inverse, from the homogeneous model to the Plücker model.

**Table 1:** The multiplication table of the inner product for the Plücker model on the null basis.

$\cdot$	$e_{01}$	$e_{02}$	$e_{03}$	$e_{23}$	$e_{31}$	$e_{12}$
$e_{01}$	0	0	0	1	0	0
$e_{02}$	0	0	0	0	1	0
$e_{03}$	0	0	0	0	0	1
$e_{23}$	1	0	0	0	0	0
$e_{31}$	0	1	0	0	0	0
$e_{12}$	0	0	1	0	0	0

$\mathbb{R}^{4,0}$ , the bracket construction is the same as dualization with respect to the pseudoscalar. This metric gives the multiplication table of table 1. Because each of its basis elements correspond to a null vector, this basis is called the null basis. Li and Zhang show that each null vector of this space satisfies the Plücker identity, and thus correspond to a line. Let  $a$  be a vector in this model.  $a$  is a line if and only if

$$\begin{aligned}
\text{Em}(a \cdot a) &= [\text{Em}(a) \wedge \text{Em}(a)] \\
&= [2(a_{01}a_{23}e_0\mathbf{e}_1 \wedge \mathbf{e}_2\mathbf{e}_3 + a_{02}a_{31}e_0\mathbf{e}_2 \wedge \mathbf{e}_3\mathbf{e}_1 + a_{03}a_{12}e_0\mathbf{e}_3 \wedge \mathbf{e}_1\mathbf{e}_2)] \\
&= 2(a_{01}a_{23} + a_{02}a_{31} + a_{03}a_{12}) \\
&= 2(a_{01}\mathbf{e}_1 + a_{02}\mathbf{e}_2 + a_{03}\mathbf{e}_3) \cdot (a_{23}\mathbf{e}_1 + a_{31}\mathbf{e}_2 + a_{12}\mathbf{e}_3) \\
&= 2\mathbf{d} \cdot \mathbf{m} \\
&= 2\Omega_q(A),
\end{aligned}$$

with  $A = \{\mathbf{d} : \mathbf{m}\}$  the corresponding Plücker coordinate representation of  $a$ . This inner product corresponds to the bilinear form  $\Omega$ .

Li and Zhang also show that the 6D space has the metric structure of  $\mathbb{R}^{3,3}$ . To demonstrate this structure, we give a second basis:

$$\{a_+, b_+, c_+, a_-, b_-, c_-\} = \left\{ \frac{e_{01} + e_{23}}{\sqrt{2}}, \frac{e_{02} + e_{31}}{\sqrt{2}}, \frac{e_{03} + e_{12}}{\sqrt{2}}, \frac{e_{01} - e_{23}}{\sqrt{2}}, \frac{e_{02} - e_{31}}{\sqrt{2}}, \frac{e_{03} - e_{12}}{\sqrt{2}} \right\}.$$

Without changing the semantics of the inner product, we obtain the multiplication table of table 2. It is apparent that the metric structure is  $\mathbb{R}^{3,3}$ ; three basis vectors,  $a_+, b_+, c_+$ , square to 1, while the other three basis vectors,  $a_-, b_-, c_-$  square to  $-1$ .

**Table 2:** The multiplication table of the inner product for the Plücker model on the screw basis.

$\cdot$	$a_+$	$b_+$	$c_+$	$a_-$	$b_-$	$c_-$
$a_+$	1	0	0	0	0	0
$b_+$	0	1	0	0	0	0
$c_+$	0	0	1	0	0	0
$a_-$	0	0	0	-1	0	0
$b_-$	0	0	0	0	-1	0
$c_-$	0	0	0	0	0	-1

It is also clear that the basis elements do not represent lines, as no basis vector squares to 0. Section 3 demonstrates that all non-null vectors of the Plücker model represent screw axes.

This screw basis is good to demonstrate the metric structure of the model. However, the null basis makes the connection to the homogeneous model more transparent.

### 2.2.1 Intersecting lines

The classical approach of linear algebra [9] gives a formula to test if two lines  $L_1 = -\{\mathbf{d}_1 : \mathbf{m}_1\}$ ,  $L_2 = -\{\mathbf{d}_2 : \mathbf{m}_2\}$  are coplanar:  $\mathbf{d}_1 \cdot \mathbf{m}_2 + \mathbf{d}_2 \cdot \mathbf{m}_1 = 0$ . This expression can be translated to our model:

$$\begin{aligned}
0 &= \mathbf{d}_1 \cdot \mathbf{m}_2 + \mathbf{d}_2 \cdot \mathbf{m}_1 \\
&= (d_{1,1}m_{2,1} + d_{1,2}m_{2,2} + d_{1,3}m_{2,3}) + (d_{2,1}m_{1,1} + d_{2,2}m_{1,2} + d_{2,3}m_{1,3}) \\
&= d_{1,1}m_{2,1} + d_{1,2}m_{2,2} + d_{1,3}m_{2,3} + m_{1,1}d_{2,1} + m_{1,2}d_{2,2} + m_{1,3}d_{2,3} \\
&= d_{1,1}e_{01} \cdot m_{2,1}e_{23} + d_{1,2}e_{02} \cdot m_{2,2}e_{31} + d_{1,3}e_{03} \cdot m_{2,3}e_{12} \\
&\quad + m_{1,1}e_{23} \cdot d_{2,1}e_{01} + m_{1,2}e_{31} \cdot d_{2,2}e_{02} + m_{1,3}e_{12} \cdot d_{2,3}e_{03} \\
&= \mathbf{E}m^{-1}(\mathbf{d}_1e_0 + \mathbf{m}_1 \rfloor \mathbf{I}_3) \cdot \mathbf{E}m^{-1}(\mathbf{d}_2e_0 + \mathbf{m}_2 \rfloor \mathbf{I}_3) \\
&= l_1 \cdot l_2,
\end{aligned} \tag{4}$$

with  $l_1, l_2$  the null vectors of the Plücker model corresponding to  $L_1, L_2$ . This test for coplanarity is a projective interpretation of intersection. That is, even two parallel lines have an intersection. This “point” of intersection  $\mathbf{p}$  is at infinity, and  $\mathbf{p} \cdot e_0 = 0$ . Projectively, points at infinity are not any different from other points.

This test for intersection also gives a geometric interpretation to the inner product of the Plücker model.

The point of intersection itself cannot easily be computed in the Plücker model, as it has no direct representation of points. Therefore, we will use the

embedding function to the homogeneous model. This lets us compute the point of intersection by the meet of  $\text{Em}(l_1)$  and  $\text{Em}(l_2)$  [4, Section 11.7.1]:

$$\begin{aligned} p &= \text{Em}(l_1) \cap \text{Em}(l_2) \\ &= (\text{Em}(l_2)^* \wedge \text{Em}(l_1)^*)^{-*}. \end{aligned} \tag{5}$$

This works for the cases of intersecting in both finite and infinite points; infinite points in the homogeneous model are represented as purely Euclidean vectors.

Together with the test for coplanarity, this can be used to see if two lines are parallel:  $(l_1 \cdot l_2)(p \cdot e_0) = 0$ . In classical literature [9], one finds a similar test, although both lines need to be decomposed into their direction and moment vectors:

$$\begin{aligned} 0 &= \mathbf{d}_1 \times \mathbf{d}_2 \\ &= (\mathbf{d}_1 \mathbf{d}_2) \rfloor \mathbf{I}_3. \end{aligned}$$

### 3 Classifying and parameterizing elements of different geometric interpretations

Before an implementation of a visualization can be made for a model, the geometric aspects of the elements of the model must be investigated. A full inventory of the geometric elements has been done [8, Chapter 3], but in different terms. Those terms are traditional, but do not hint at the geometric concept. Besides the traditional terms, geometric inspired terms will be used.

The following sections will discuss the geometrically different blades of a certain grade, together with their duals. The discussion of  $(n > 1)$ -blades is limited to those composed of null vectors. Visual representations of the analyzed elements are presented in appendix A.

#### 3.1 Blades of grade 0 and 6

Scalars and pseudoscalars are interpreted the same as in other models for geometric algebra. Scalars can be used to represent weights. Its dual, the pseudoscalar, may be utilized to denote the subspace volume.

#### 3.2 Blades of grade 1 and 5

We will distinguish three classes based on geometric interpretation. For all three classes, their direction and moment are algebraically the same; these components are only interpreted differently in the domain of geometric interpretation. The weight is computed as well in a uniform way, again through the homogeneous model:

$$w(x) = w(\text{Em}(x)) = \sqrt{(\text{Em}(x) \rfloor -e_0)^2 + (\text{Em}(x) \rfloor \mathbf{I}_3^{-1})^2}$$

For non-null vectors, the weight can also be computed as  $\sqrt{x \cdot x}$ . In the general case of a  $k$ -blade  $x_1 \wedge \cdots \wedge x_k$ , we define its weight as

$$w(x_1 \wedge \cdots \wedge x_k) = w(\text{Em}(x_1)) \cdots w(\text{Em}(x_k)).$$

It is clear from subsection 2.2 that the null vectors of the Plücker model (those vectors  $v$  satisfying the Plücker identity  $\Omega_q(v) = 0$ ) are interpreted as lines. Let  $l = d_1 e_{01} + d_2 e_{02} + d_3 e_{03} + m_1 e_{23} + m_2 e_{31} + m_3 e_{12}$  be a null vector. The line can be interpreted through the homogeneous model. The direction of the line corresponds to  $(\text{Em}(l) \rfloor -e_0)/w(l)$ , while its moment is  $(\text{Em}(l) \wedge e_0)^*/w(l) = (\text{Em}(l) \rfloor (e_0 \rfloor (e_0 \mathbf{I}_3)^{-1}))/w(l) = (\text{Em}(l) \rfloor \mathbf{I}_3^{-1})/w(l)$ .

A special case are the ideal lines. The homogeneous model allows two interpretations. Its first, and most common interpretation is a 2D direction, the same interpretation as it is given in the Euclidean model. For the second interpretation, we have to look a bit closer at the homogeneous model. A

homogeneous line can be defined as the outer product of two homogeneous points. A homogeneous point  $a = \mathbf{a} + \alpha e_0$  has location  $\mathbf{a}/(e_0 \cdot a)$ . In the case of ideal lines, we are dealing with points of the form  $a = \lim_{\alpha \rightarrow 0} \mathbf{a} + \alpha e_0$ . Its location then becomes  $\lim_{\alpha \rightarrow 0} \mathbf{a}/(e_0 \cdot a) = \infty$ . Because  $\mathbf{a}$  is not depending on  $\lim_{\alpha \rightarrow 0} e_0 \cdot a$ , the model allows more than one point on that location, each with a different direction.<sup>3</sup> Lines of two of these points at infinity are at infinity as well. One can visualize such an ideal line  $l_\infty = m_1 e_{23} + m_2 e_{31} + m_3 e_{12}$  as a horizon, a circle on the celestial sphere in direction  $(Em(l_\infty) \wedge e_0)^*/w(l)$ . We will use this last interpretation as the default interpretation. When the 2D direction interpretation is used, it will be explicitly stated.

The vectors that do not square to 0 can be interpreted as the axis of a helical, or screw motion [8, Section 3.1.2]. A screw motion simultaneously translates and rotates an object. The object is translated along the same line as around which the rotation is performed. The motion can be fully characterized by this line  $a$  and the pitch  $p$ , the amount of translation per rotation. For the grade 5 screw motion  $S = \{\mathbf{d} : \mathbf{m}\}^*$ , its pitch and axis are given by [8, Theorem 3.1.9]:

$$\begin{aligned} p &= \mathbf{d} \cdot \mathbf{m} / \mathbf{d}^2 \\ a &= \{\mathbf{d} : \mathbf{m} - p\mathbf{d}\}. \end{aligned} \tag{6}$$

From this, one can deduce what kind of objects the dual elements of real and ideal lines represent. For an ideal line  $l_\infty$  with  $p = \lim_{\mathbf{d} \rightarrow 0} \mathbf{d} \cdot \mathbf{m} / \mathbf{d}^2 = \infty$  and  $a = \lim_{\mathbf{d} \rightarrow 0, p \rightarrow \infty} \{\mathbf{d} : \mathbf{m} - p\mathbf{d}\} = l_\infty$ , we see that it is a pure translation. Given a real line  $l_o$ , its pitch is  $p = 0 / \mathbf{d}^2 = 0$ , because of the Plücker identity, seen in equation 2. Its axis is  $a = \{\mathbf{d} : \mathbf{m} - 0\} = l_o$ . No matter how much of the rotation is applied, no translation will occur. This shows that the dual of real lines represent pure rotational motions.

### 3.3 Blades of grade 2 and 4

A 2-blade  $B = a \wedge b$  represents the set of linear combinations of  $a$  and  $b$ :

$$\mathcal{C} = \{c \mid c \wedge B = 0\} = \{\lambda a + \mu b \mid \lambda, \mu \in \mathbb{R}\}.$$

For the geometric interpretation of these blades, clarity on what kind of objects are in this set is needed. On first inspection, this can be split in three cases, based on the number of null vectors among the factors. We will limit this discussion to the case where both  $a$  and  $b$  are null vectors.

---

<sup>3</sup>A similar definition found in other sources [4, Section 11.3] is  $a = \lim_{\|\mathbf{a}\| \rightarrow \infty}$ . This avoids division by zero, but is less appropriate in our case.

A linear combination  $c = \lambda a + \mu b$  is a null vector if:

$$\begin{aligned} c^2 &= (\lambda a + \mu b) \cdot (\lambda a + \mu b) \\ &= \lambda^2 a^2 + 2\lambda\mu a \cdot b + \mu^2 b^2 \\ &= 2\lambda\mu a \cdot b \end{aligned} \tag{7}$$

When  $a$  and  $b$  are coplanar (that is, they intersect or are parallel), their inner product is zero (see equation 4), and each linear combination  $c = \lambda a + \mu b$  is a null vector. This kind of object is called a pencil of linear line complexes [8, Section 3.2.1], or, a bit shorter, a pencil of lines [7].

The homogeneous point in which all lines intersect, is called its center [7], and can be computed, as seen in equation 5. The bivector direction containing the pencil can be computed by:

$$\begin{aligned} \mathbf{D} &= (\text{Em}(a) \rfloor e_0) \wedge (\text{Em}(b) \rfloor e_0) \\ &= \mathbf{d}_a \wedge \mathbf{d}_b \end{aligned}$$

This has no practical results when  $a$  and  $b$  are parallel. When they are parallel,  $\text{Em}(a) \rfloor e_0$  differs from  $\text{Em}(b) \rfloor e_0$  only in a scalar factor, and therefore their outer product is 0. The intersection of  $a$  and  $b$  happens at a point at infinity. For visualizations, it proves useful to know the pencil's bivector direction, as well as a finite point on the pencil.

As discussed, the intersection of two parallel lines results in a Euclidean vector, which can be interpreted as either a point at infinity in the homogeneous model, or a direction in the Euclidean model. We can define the bivector direction of a pencil of parallel lines as:

$$\mathbf{D} = (\text{Em}(a) \cap \text{Em}(b)) \wedge (p_b - p_a)$$

Often one takes the point on the object closest to the chosen origin. For a line  $l = \{\mathbf{d} : \mathbf{m}\}$ , this is given by  $p = \mathbf{m} \times \mathbf{d} + \mathbf{d}^2 e_0$  [9]. Let  $p_a$  and  $p_b$  be such points for  $a$  and  $b$ . The homogeneous line  $C = p_a \wedge p_b$  is the line that intersects each line in their point closest to the origin. We define a third point  $p_C$  that is the point nearest the origin and on  $C$ . This point lies on line  $C$ , as well as on a line contained by  $B$ , as  $C$  contains the point nearest the origin of each line in  $B$ .

The dual of a pencil of lines contains the same set of lines [8, Section 3.2.1]. This can be easily shown. Stating the definition of  $\mathcal{C}$  differently, we are looking for all lines that are contained in  $B$ . This is expressed as  $c \wedge B = 0$ . For the grade-4 object  $B^*$ , this can be written as  $c \rfloor B^* = c \rfloor (B \rfloor I_6^{-1}) = (c \wedge B) \rfloor I_6^{-1}$ , with  $I_6$  the pseudoscalar of the space  $\mathbb{R}^{3,3}$ . This is only true for  $c \wedge B = 0$ , a test for containment of  $c$  in  $B$ .

Now look at the case where  $a$  and  $b$  are not coplanar, but  $a \wedge b$  still contains lines. equation 7 shows that either  $\lambda = 0$  or  $\mu = 0$ , as  $a \cdot b \neq 0$



per definition. This means that all null vectors in  $\mathcal{C}$  must be homogeneously equivalent to  $a$  or  $b$ . This class of geometric objects is known as the hyperbolic linear congruence. Its dual, the hyperbolic pencil of linear complexes, contains all lines intersecting both  $a$  and  $b$  [8, Proposition 3.2.3]. That is, for each point  $p_a$  on  $a$  and  $p_b$  on  $b$ , the line  $c$  with embedding  $\text{Em}(c) = p_a \wedge p_b$  is in  $B^*$ .

Now that we have handled the cases where  $a$  and  $b$  are both null-vectors, we will investigate the case where .

### 3.4 Blades of grade 3

When talking about three lines  $a, b, c$  in 3D space, we can distinguish several cases:

- Case 1. All lines are pairwise coplanar and intersect in a single point. This is called a 2D concurrent pencil or point [7].
- Case 2. All lines are pairwise coplanar but intersect in three different points. Li and Zhang name this object a 2D coplanar pencil, or plane [7].
- Case 3. One line is coplanar to the other two lines, which are not coplanar to each other. This is a couple-wheel pencil [7].
- Case 4. No line is coplanar to the other lines. The geometric entity is named a regulus [8, Section 3.3].

Unlike blades of other grades, the dual of a 3-blade  $B = a \wedge b \wedge c$  is  $-B$ ; when dualized, only the orientation of the 3-blade is switched. From here on, we will not give any attention to the duals of the 3-blades.

We will only discuss the first three geometric cases. The last case defines the reguli, a class of hyperboloid and paraboloid ruled surfaces. We do not treat them here, because of time constraints on the project and expected involved computations of the set of contained lines. Let  $x$  be the axis around which the lines of the regulus  $R$  are placed,  $p$  a plane perpendicular to  $x$ ,  $p_x$  the point where  $x$  intersects  $p$ , and  $\mathcal{P}_R$  the set of intersection points of  $p$  with the lines in  $R$ . We expect that the Euclidean distance between  $p_x$  and  $p_R \in \mathcal{P}_R$  is not constant for all points in  $\mathcal{P}_R$ . That is, for a general regulus  $R$ , we expect that  $\mathcal{P}_R$  describes an ellips. For this we need to analyze the reguli better, which did not fit in the scope of this project.

Similar to the 2-blades, a 3-blade  $B = a \wedge b \wedge c$  represents the set of linear combinations of  $a$ ,  $b$  and  $c$ :

$$\mathcal{D} = \{d \mid d \wedge B = 0\} = \{\lambda a + \mu b + \nu c \mid \lambda, \mu, \nu \in \mathbb{R}\}.$$

A linear combination  $d = \lambda a + \mu b + \nu c$  is a null vector if:

$$\begin{aligned}
d^2 &= (\lambda a + \mu b + \nu c) \cdot (\lambda a + \mu b + \nu c) \\
&= (\lambda a + \mu b) \cdot (\lambda a + \mu b) + (\lambda a + \mu b) \cdot \nu c + \nu c \cdot (\lambda a + \mu b) + \nu c \cdot \nu c \\
&= 2(\lambda \mu a \cdot b + (\lambda a + \mu b) \cdot \nu c) \\
&= 2(\lambda \mu a \cdot b + \lambda \nu a \cdot c + \mu \nu b \cdot c).
\end{aligned}$$

For the first two cases we have  $a \cdot b = a \cdot c = b \cdot c = 0$ , and thus all linear combinations of  $a$ ,  $b$  and  $c$  are in  $\mathcal{D}$ . Their points of intersecting are given by  $p_{ab} = \text{Em}(a) \cap \text{Em}(b)$ ,  $p_{bc} = \text{Em}(b) \cap \text{Em}(c)$ ,  $p_{ca} = \text{Em}(c) \cap \text{Em}(a)$ . Projectively, cases 1. and 2. are equivalent (the point of intersection is not a projective property, but coplanarity is), but their geometric interpretation differs.

The case of three lines intersecting in a single point can be seen as a 3D pencil of lines. Given a pencil of lines  $a \wedge b$ , we take the outer product with a third line  $c$  that goes through the center of the pencil. This bundle of lines can be used to represent a point, as it is rotation-invariant. We have already computed the location of this point; it is the same as the center of  $a \wedge b$ , as  $p_{ab} = p_{bc} = p_{ca}$  per definition.

When three lines are parallel to each other, their meet results in a Euclidean vector. Just like ideal lines, these elements can be interpreted in two ways. One way is to look at it as a direction, similar to the Euclidean interpretation. The homogeneous model gives us the interpretation of a point infinitely far away. This interpretation is an extension of the notion of a point. Let  $a = \lim_{\alpha \rightarrow 0} \mathbf{a} + \alpha e_0$  be a point in the homogeneous model. Its location is computed by  $\lim_{\alpha \rightarrow 0} a / (e_0 \cdot a) = \infty$  [4, Section 11.2]. Both interpretations are correct, however incomplete. In our interpretation, lines do not only intersect at  $a$  on the celestial sphere, but also in  $-a$ . Because all elements extend infinitely, they intersect the celestial sphere twice. This point pair-like characteristic can also be observed when defining ideal points on the celestial sphere. There we can define an ideal point as the intersection of two horizons. When visualized, it becomes clear that the horizons intersect twice.

The second case states that  $a$ ,  $b$  and  $c$  intersect each other in three different points. Again, any linear combination of  $a$ ,  $b$  and  $c$  is contained by  $\mathcal{D}$ , but this represents a plane;  $\mathcal{D}$  contains all lines in direction  $\mathbf{D} = \frac{1}{3} \mathbf{d}_a \wedge \mathbf{d}_b + \mathbf{d}_b \wedge \mathbf{d}_c + \mathbf{d}_c \wedge \mathbf{d}_a$ . Because  $p_{ab}$ ,  $p_{bc}$  and  $p_{ca}$  lie in the same plane, we compute the location of  $B$  in the same way as it is computed for  $p_{ab} \wedge p_{bc} \wedge p_{ca}$ .

The outer product of the three ideal lines span an ideal plane. In our celestial sphere interpretation, they represent the sphere itself. In the interpretation of the Euclidean directions, as well as the homogeneous model, it corresponds with the Euclidean pseudoscalar.

The third case describes a pair of line pencils, joined through a single common line. Let  $b$  be the connecting line of the two pencils:  $a \cdot b = b \cdot c = 0$  and  $a \cdot c \neq 0$ . The null vectors of  $\mathcal{D}$  are exactly those contained by the set of linear combinations of  $a \wedge b$  and  $b \wedge c$ .

Because  $b$  intersects both  $a$  and  $c$ , we can rewrite  $d^2 = 0$  as  $\lambda \nu a \cdot c = 0$ . This only holds for  $\lambda = 0$  or  $\nu = 0$ .  $\mathcal{D}$  corresponds with the union of sets of lines  $\mathcal{L}_{ab}$ ,  $\mathcal{L}_{bc}$ ,  $\mathcal{L}_{ca}$  for respectively  $a \wedge b$ ,  $b \wedge c$  and  $c \wedge a$ :

$$\begin{aligned}
\mathcal{L}_{ab} \cup \mathcal{L}_{bc} \cup \mathcal{L}_{ca} &= \{\lambda a + \mu b\} \cup \{\mu b + \nu c\} \cup \{\nu c + \lambda a \mid \nu = 0 \vee \lambda = 0\} \\
&= \{\lambda a + \mu b\} \cup \{\mu b + \nu c\} \\
&= \{\lambda a + \mu b + \nu c \mid \nu = 0\} \cup \{\lambda a + \mu b + \nu c \mid \lambda = 0\} \\
&= \{\lambda a + \mu b + \nu c\} \\
&= \mathcal{D},
\end{aligned}$$

with  $\lambda, \mu, \nu \in \mathbb{R}$ .

## 4 Implementation

With the knowledge of the frameworks acquired in section 2 and section 3, we now can extend the functionality of GAViewer. The following parts will discuss the following subjects: how GAViewer can be extended, and how it has been done; the origins of the software for computing with the Plücker model; how casting from and to the Plücker model is realized; and, lastly, the visualization of each provided element is explained.

### 4.1 Software design decision

Extending GAViewer's functionalities can be done in two ways.

Since version 0.4, GAViewer can open a TCP port for communication with other programs [5]. The extended functionality can be implemented by a program that maintains an own interface for user input. The input will be sent to GAViewer over a TCP port, after it has been processed by the new application. Textual results are returned over the TCP port, and thus can be shown in the application's own user interface. However, the visualization of the elements will be shown in GAViewer's own viewport. The user has to switch between user interfaces to view textual or visual representations, which the user probably experiences as confusing or annoying. To show the new model's blades correctly, it should be possible to characterize their visualization in terms of elements of other models, and elements of those models should be passed around between the new program and GAViewer. This limitation seems undesired for our elements; no supported model has primitives that can make up a screw axis' visualization.

Users want to interact with the drawn elements in GAViewer. This means that their transformations will have to be translated to corresponding transformations of our model. All objects, like a pencil of lines, will have to be drawn by a set of elements of an existing model. This complexity grows when such elements of the new model are declared dynamic; a whole net of interdependencies arises. We would rather avoid code complexity, as that often gives rise to bugs.

The C++ source code of GAViewer is freely available on the internet<sup>4</sup>. This means that GAViewer could also be extended by adding the new functionality in the original source code, and compile it all together to form a unified piece of software. Because there is very little documentation in the source code on how to extend the functionality of GAViewer with a new model, an old model that has gone out of use might be replaced with our new one. With a textual search through the source code, it is possible to find all hooks for adding the right functionality.

---

<sup>4</sup>The source code of GAViewer can be downloaded from [http://geometricalgebra.net/gaviewer\\_download.html](http://geometricalgebra.net/gaviewer_download.html).

The problems that arose from extension through an external implementation do not apply. The unified user interface can be taken for granted. User interaction and dynamic statement management are all implemented independent from the models. Only the transformation resulting in the new object when dragged has to be implemented once. This is easy to do for all elements, because our model is operational. New graphical elements can be made when needed, because calls to OpenGL routines can be made.

We have decided to remove the existing 6D model for `i2ga` and substitute it with our new model, named `13ga`. No element of `i2ga` currently has visualizations and after a short interview, interest in `i2ga` within the user base of GAViewer has dropped. The original developer warned that adding a new model might raise unknown bugs; although the program has been made with the idea that it might be extended some day, it has not been thoroughly tested or documented.

## 4.2 Computing with 13ga in GAViewer

GAViewer relies on code generated by Gaigen for the implementation of each model [6]. Although more recent versions of Gaigen, such as version 2.5, have a better performance, the code for `13ga` has been generated by the same version of Gaigen, version 1.0, which generated the other models as well. This has three reasons. The API of more recent versions are not compatible with the API of the version used by the application. The documentation of GAViewer states that it is inappropriate to use GAViewer in applications that need good performance, as the internal, interpreted programming language is too slow and limited [5, page 7]. Therefore, performance improvements in only a model would not suffice to make the program more useful. Furthermore, the used implementations are fast enough to handle hand-typed expressions without any noticeable delay for the user.

## 4.3 Models and casting

The geometric interpretation of an object of geometric algebra is based on its model. When an expression is evaluated without any explicit model specifier, GAViewer will try to evaluate it in the model of `e3ga` first. If the expression contains terms of a different model, GAViewer automatically applies the appropriate model. In case there are terms that cannot be interpreted in any model, those evaluate to 0.

GAViewer has support for casting objects from one model to another. Multivectors are expressed on the source model's basis, and corresponding basis vectors of the target model are multiplied by the source model's factors. For example, the expression  $3.00 \cdot \mathbf{e1} \wedge \mathbf{e5} + 0.50 \cdot \mathbf{e3} \wedge \mathbf{no}$  evaluates to an object of model `c5ga`. When cast to `c3ga` it evaluates to  $0.50 \cdot \mathbf{e3} \wedge \mathbf{no}$ , as `c3ga` does not have a vector that has similar semantics to `e5`. Casting to

**Table 3:** GAViewer uses colors to encode the grade of the object.

Grade	Color
0	Black
1	Red
2	Blue
3	Green
4	Yellow
5	White
6	Red

$p3ga$  results in  $0.50 * e3^e0$ , because the semantics of  $no$  and  $e0$  correspond; both represent an arbitrarily chosen origin. Casting to  $e3ga$  results in 0, as both  $e1^e5$  and  $e3^no$  cannot be interpreted in the model.

The casting from  $l3ga$  to  $p3ga$  has been implemented in the same way as expressions from the Plücker model are embedded in the homogeneous model through the embedding function  $Em$ , defined in equation 3. The casting to other models is equivalent to casting to  $p3ga$ , and then to the target model.

Casting to  $l3ga$  has been done in a corresponding way. As a consequence, only even grade terms of a multivector can be cast from the current models to  $l3ga$ . The objects  $e1^e2^e3^e0$  from  $p3ga$  and  $e1^e2^e3^no$  from  $c3ga$  and  $c5ga$ , are algebraically equivalent to  $-e01^e23$ ,  $-e02^e31$  and  $-e03^e12$ . This ambiguity has been resolved by returning the sum of all these three blades, divided by 3. In addition, a warning text is presented to the user, stating this.

#### 4.4 Blade interpretation and visualization

Section 3 discusses several classes of blades with their geometric interpretation. In this section, the computations of the position and stance of these blades in 3D space are given, together with a motivation for the chosen visualization.

GAViewer provides user controlled switches for visualizing the object's orientation and weight. How these properties of the object are displayed is discussed as well.

In the visualization, the grade of the object is shown through usage of certain colors. This association of color and grade is given in table 3. Note that grade 1 and grade 6 objects share the same color; during the original design of GAViewer, no grade 6 objects were expected to be visualized.

#### 4.4.1 Grade 0

GAViewer does not visualize scalars for the originally implemented models, `e3ga`, `p3ga`, `c3ga`, `c5ga`, and `i2ga`. With `l3ga`, we have decided to follow this example. It adds a piece of consistency in the interface of the application. When no explicit casting is done, objects are cast to the simplest model that contains the object. Scalars are thus identified as part of `e3ga`. When they are cast to `l3ga`, it is consistent not to display the object, as no geometric semantics of this element have changed.

#### 4.4.2 Grade 1

1-blades can be either a real line, an ideal line or a screw axis. Each class needs to be interpreted slightly differently.

**4.4.2.1 Real line** Real lines have a weight, orientation and a location. The direction vector  $\mathbf{d}$  as mentioned in subsection 2.2 determines the line's orientation. To determine its orientation properly, the software uses the normalized direction  $\mathbf{d}/\|\mathbf{d}\|$ .

The location is standardized to be the point closest to the origin of GAViewer's drawing area. The classical literature on Plücker coordinates [9] presents a way to parameterize the homogeneous points on a line  $-\{\mathbf{d}, \mathbf{m}\}$ . This parametrization is given by  $p(t) = \mathbf{m} \times \mathbf{d} + t\mathbf{d} + \mathbf{d}^2 e_0$ . For  $t = 0$ , the normalized point nearest to the origin is  $(\mathbf{m} \times \mathbf{d})/\mathbf{d}^2$ .

Real lines are represented similarly to the lines of `p3ga`, `c3ga` and `c5ga`; a solid line with optional orientation marks. The length of the marks are a visual clue of the weight. Although the mathematical object is infinitely long, the length of the lines drawn are limited by a constant, internally defined in GAViewer.

**4.4.2.2 Ideal line** Ideal lines cannot be characterized in this way as  $\mathbf{d} = 0$  per definition. They have no specific location (each point on an ideal line is infinitely far away from any other non-ideal point). That means that  $\mathbf{m}$  represents an ideal line's orientation.

The orientation of an ideal line  $L$  can be seen as a direct or indirect representation. Directly, this would give us a line through the origin, in the direction of  $\text{Em}(L)^*$ , where  $\mathbf{d}_{\text{Em}(L)^*} = \text{Em}(L) \rfloor \mathbf{I}_3^{-1}$ . With this representation, ideal lines are displayed the same way as real lines, except that the line is dotted to show the difference.

In the indirect representation, the ideal line could be represented as a circle on the celestial sphere, where the orientation acts as the ideal line's normal. This agrees with the interpretation of ideal lines as horizons. However, it is hard to make clear for the user that the circle is indeed on the celestial sphere, when other elements are not. To eliminate confusion with

genuine finite circles, which would otherwise be drawn similar, GAViewer draws celestial circles as a dotted finite circle at the origin. The orientation is represented by hooks attached on the circle. Weight can be visualized either by the length of the marks, or by varying the radius of the circle.

Ideal lines are not represented by the same visualization as **e3ga**'s bivectors are, even though they have a more directional aspect than the other vector classes. This has been done to make clear that these objects represent lines nonetheless, and are fundamentally different from **e3ga**'s bivectors, even when an ideal line can be cast to such a bivector.

**4.4.2.3 Screw axis** The axes of screw motions have two visualizations. By default, only one period is shown. The screw axis is shown as a spiral, with its pitch determining the length of the spiral. With a positive pitch, the spiral performs a right-handed rotation. In case of a negative pitch, the spiral is left-handed. The orientation of the screw axis is given by the orientation of its axis (see equation 6), and visually represented by a vector's arrow head on the corresponding end of the spiral. Its weight can be shown visually by the radius of the spiral.

As an alternate visualization, the user can choose to show a whole column of joined spirals.

### 4.4.3 Grade 2

The visualization of the pencil of linear line complexes, and the hyperbolic linear congruence are provided.

**4.4.3.1 Pencil of linear line complexes** Pencils of real, not parallel lines are visualized as a sample of the lines contained by the blade. For the pencil of real lines  $B = a \wedge b$ , 64 evenly distributed line pieces of length  $w(B)$  are drawn that intersect at the center of  $B$ . We have chosen to limit the sample to this number of line pieces, as the interface might get cluttered. We draw line pieces instead of full lines with the same reason. If the user desires to have the orientation visualized, the line pieces are replaced with four times fewer vectors of the same length. For a positive orientation, the vectors point to the center. For a negative orientation, the vectors point the other way.

In case of a pencil of real, parallel lines, a set of parallel lines in direction  $\mathbf{D} = (\text{Em}(a) \rfloor -e_0) \wedge (\text{Em}(b) \rfloor -e_0)$  are drawn. This set has the same dimensions as the implemented visualization of a plane. Given the width of the drawn plane  $w$ ,  $5w$  lines are drawn. Weight and orientation are drawn in the same way as it is drawn for planes; normal lines appear on one side of the pencil, their direction representing the orientation, and their length representing the weight.



When the pencil contains only ideal lines, 32 evenly distributed ideal lines in the horizon representation are drawn. These result in a set of rotated circles. If the orientation is displayed, a vector is drawn on either of the intersection of the circles, pointing at the other intersection.

**4.4.3.2 Hyperbolic linear congruence** The 2-blade of two lines that are not coplanar contains only these two lines. We only draw these two lines for their visualization. These lines can be both real, or one real and one ideal. To indicate the orientation in the case of two real lines, a vector is drawn between the points nearest to the origin of both lines, as well as the hooks that are default for lines. If the blade contains one real and one ideal line, only the hooks are displayed.

The weight is visualized by the size of the hooks.

#### 4.4.4 Grade 3

We have implemented visualization routines for the points, planes and the couple-wheel pencils. As we have not analyzed the reguli, we do not supply visualization routines.

**4.4.4.1 Point** We draw the blades of three concurrent points with the same routines as points of the homogeneous and conformal models. Consistent with the points of other models, the orientation is not visualized. Its weight is visualized through the size of the point.

An ideal point is visualized as a pair of dotted points. When the user wants to see the orientation, a dotted vector is drawn from one point to the other. The user is informed of the ideal point's weight by the distance between the two graphical points.

**4.4.4.2 Plane** The visual representation of planes of the Plücker model is generated in the same way as for planes in other models. When required by the user, the weight is represented by the length of normal lines on one side of the plane. The side chosen is determined by its orientation.

Because we can see the ideal plane as the celestial sphere, we draw it as a dotted sphere. The weight is represented by the sphere's radius, while its orientation is represented in the same way as it is done for the real plane. This visualization equals that of the Euclidean trivector, which is another interpretation of the ideal plane.

**4.4.4.3 Couple-wheel pencil** The couple-wheel pencil is visualized by the visualization of its two pencils, joined together with a line piece between the two centers. The weight is visualized through the length of the line pieces of the two pencils. When the orientation should be visualized, the line piece representing the common line is replaced by a vector.

#### 4.4.5 Grade 4

Just as their duals, the dual pencil of linear line complexes as well as the hyperbolic pencil of linear complexes are provided with visualizations.

**4.4.5.1 Dual pencil of linear line complexes** Pottmann and Wallner show that the dual of a pencil of linear line complexes contains the same lines as its direct representation [8, Section 3.2.1]. Therefore, the computations needed for the visualizations are done with the dual element. The visual representation is equivalent to that of the grade 2 element.

**4.4.5.2 Hyperbolic pencil of linear complexes** The location and orientation of a hyperbolic pencil of linear complexes is also computed with its dual, a pair of skew lines. The visualization shows a sample of the direct representation of the 4-blade. The sample takes 31 evenly spaced points on both lines of its dual, and connects them. The lines are not drawn with the same length as the grade 1 lines. We believe that this amount of long lines clutter the interface and obscures the geometrical structure of the object. The line pieces are only drawn from a point from one line to a point on the other line.

The orientation of this congruence is defined as the orientation of its dual. When the orientation is shown, the line pieces are replaced with vector objects, pointing in the same direction as the single vector points in the case of the dual.

#### 4.4.6 Grade 5

5-blades are visualized in the same way as their duals. Vectors represent the axis of the motion of a grade 5 object, and thus can give a good visual indication of the nature of the motion itself.

#### 4.4.7 Grade 6

The originally implemented models show a slight inconsistency for visualization of their pseudoscalar. While GAViewer displays a transparent sphere for `e3ga`'s pseudoscalar, the other models display nothing. As in the scalar case, we have chosen for consistency with the largest number of models supplied, and do not draw the pseudoscalar. By duality to scalars, it is safe to say that the semantics of the pseudoscalar have not changed.

### 4.5 User interaction

For the original models, most visualizations of objects in GAViewer can be dragged with a right mouse click while holding the `Ctrl` key down. The objects that can be translated, are translated corresponding to the mouse's

movement. Objects that are translation invariant, are rotated accordingly. Objects that are invariant under translation and rotation, such as the Euclidean trivector, are only scaled. Besides rotating, Euclidean vectors are scaled as well.

We have implemented this part of the user interaction for our model. The real lines, screws, pencils of real lines, line pairs, real points, real planes and couple-wheel pencils are translated. Ideal lines, pencils of ideal lines are rotated, as their geometric interpretation has no location. The ideal plane is scaled in the same way the Euclidean trivector is.

We have used the translation and rotation versors presented in an internal report [3]. Translation over  $\mathbf{t} = \tau_1 \mathbf{e}_1 + \tau_2 \mathbf{e}_2 + \tau_3 \mathbf{e}_3$  is performed by the versor  $T_{\mathbf{t}}$ :

$$T_{\mathbf{t}} = \exp\left(\frac{1}{2}(\tau_1 e_{12} \wedge e_{31} + \tau_2 e_{23} \wedge e_{12} + \tau_3 e_{31} \wedge e_{23})\right).$$

Clockwise rotation in the bivector plane  $\mathbf{R} = \rho_1 \mathbf{e}_2 \mathbf{e}_3 + \rho_2 \mathbf{e}_3 \mathbf{e}_1 + \rho_3 \mathbf{e}_1 \mathbf{e}_2$  around the origin over  $w(\mathbf{R})$  radians is performed by  $R_{\mathbf{R}}$ :

$$R_{\mathbf{R}} = \exp\left(\frac{1}{2}(\rho_1(e_{02} \wedge e_{12} - e_{03} \wedge e_{31}) + \rho_2(e_{03} \wedge e_{23} - e_{01} \wedge e_{12}) + \rho_3(e_{01} \wedge e_{31} - e_{02} \wedge e_{23}))\right).$$

## 5 Conclusion

This thesis presents a method for most blades in the space  $\mathbb{R}^{3,3}$  of the Plücker model. This has been done through an embedding function  $\text{Em}$  of the Plücker model to the homogeneous model, provided by Li and Zhang [7]. We have demonstrated that among the blades of  $\mathbb{R}^{3,3}$  are (real and ideal) lines, screw axes, pencils of linear line complexes, hyperbolic linear congruence, points, planes, couple-wheel pencils, and their duals. Most of this is done through finding correspondences between the elements of a similar model for linear algebra, employed by Pottmann and Wallner [8] and those of our algebra.

We present a function to compute the weight and orientation of each element of our algebra. We also show how necessary characteristics of the above stated geometric entities for visualization are computed.

GAViewer, a graphical calculator for various models of geometric algebra [5], has been extended with the above knowledge. Support for the algebraic model is added through code generated by Gaigen [6], although support for an algebra used to represent 2D grey value images has been dropped. GAViewer has casting operators, that work as embedding functions between other models and the Plücker model. With the computed characteristics of the elements, GAViewer generates visualizations of the described geometric entities on user input without any noticeable delay.

But there is more work to be done in both our implementation as well as in developing an understanding of the Plücker model for geometric algebra. We have only investigated the  $(n > 1)$ -blades that can be generated by the outer product of null vectors. Exploration of the other blades in this model for geometric algebra has to be done. For instance, the parabolic and elliptic pencils of linear complexes and their congruences [8, Section 3.2.1] are not demonstrated as members of the model, while they are in the similar model for linear algebra. Our visualization of the elements of grade 5 is based on their duals' interpretation, but a more direct graphical representation might be beneficial for the user's understanding of the object. The blades of grade 3 which are composed of three mutually skew lines need more analysis before they can be fully characterized.

This thesis presents no transformations, although it is claimed [7] that the model is operational. An introduction to these is given in an internal report [3]. One might investigate if it is useful for the user to have these visualized by GAViewer.

We have shown that several 1- and 3-blades correspond geometrically to specific 1-, 2- and 3-blades of the homogeneous model. A study of their relationship might reveal an embedding function of the Euclidean model in the Plücker model.

The model used is for the base space  $\mathbb{R}^3$ , and it is easy to see a similar model for any real vector space of odd dimensionality. In these other models,

even more geometric entities might rise. General relationships between these entities might be designed.

More interesting for its practical applications would be to develop a similar model for a real vector space of even dimensionality, such as  $\mathbb{R}^2$ . It might be realized within  $\mathbb{R}^{3,3}$  as the intersection with a plane, but this needs more research to see if this model has any practical significance.

## A Visualizations

This appendix contains visualizations of the analyzed blades of section 3, generated by the extended implementation of GAViewer described in section 4. The images are generated without changing the position of the viewport with respect to the origin.

For some objects, we show several differently parameterized versions to give the user an idea of how algebraic concepts are visualized.

**Figure 2:** The real line  $e_{01}$  with its orientation shown. Compare the length of the arrows with those of figure 12 for the visualization of the weight.

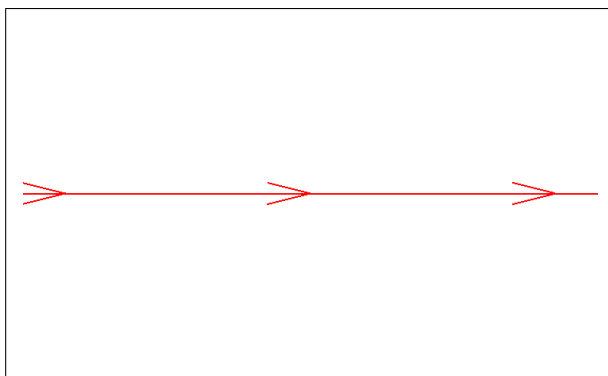


**Figure 3:** The ideal line  $e_{12}$  with its orientation shown. Its weight  $w = 1$  is displayed by the radius of the circle. Compare with figure 5 for the visualization of its weight.

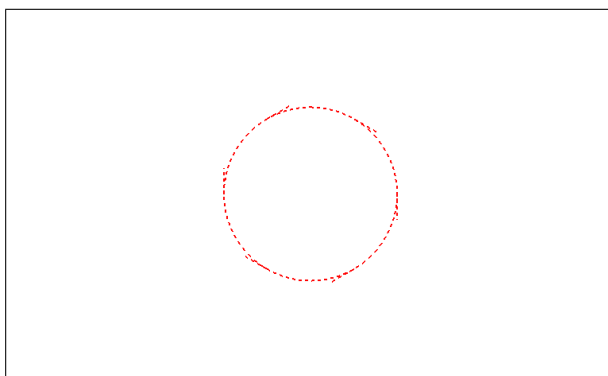


**Figure 4:** The screw  $(e_{01} + 4e_{23})/\sqrt{1^2 + 4^2}$ . Its pitch  $p = 4$  is shown by the length of the spiral.

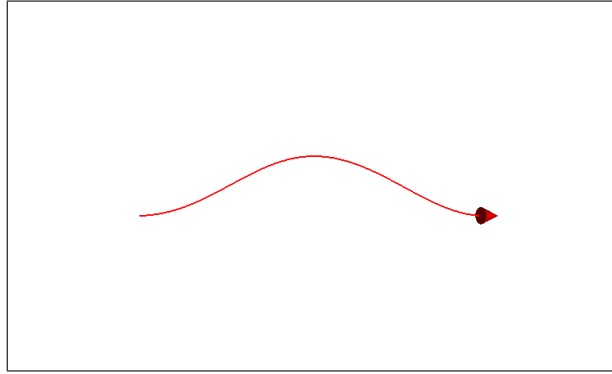


**Figure 5:** The screw  $4(e_{03} + 4e_{12})/\sqrt{1^2 + 4^2}$ . Its weight  $w = 2$  is displayed by the radius of the spiral. Compare with figure 3 for the visualization of the weight.

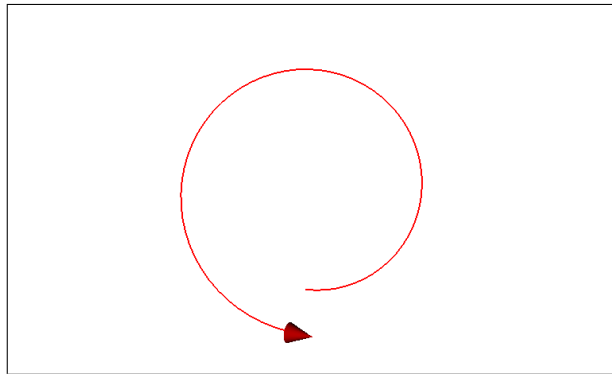


**Figure 6:** The pencil of lines  $e_{01} \wedge e_{02}$  with no orientation shown. Compare with figure 7 and figure 8 for the visualization of its weight and orientation.

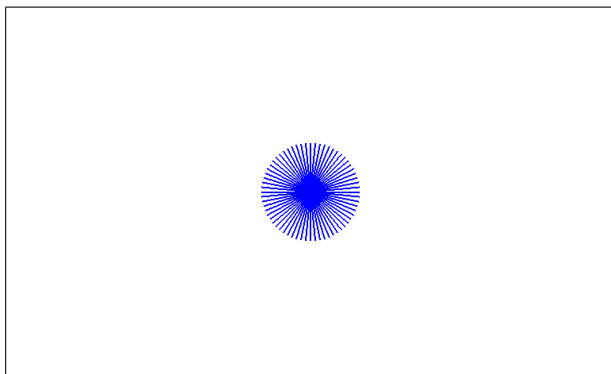


**Figure 7:** The pencil of lines  $3e_{01} \wedge e_{02}$  with its orientation shown as vectors pointing. Compare with figure 6 and ?? for the visualization of its weight and orientation.

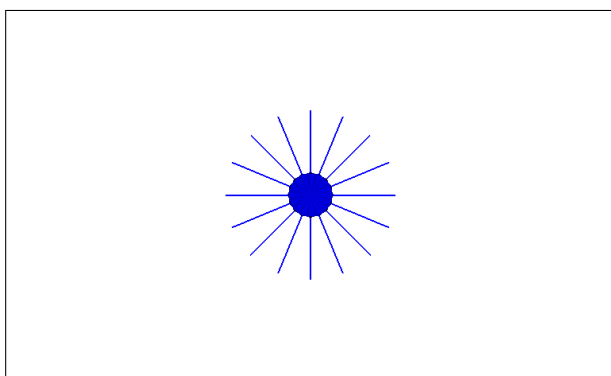




**Figure 8:** The pencil of lines  $-\frac{1}{2}e_{01} \wedge e_{02}$  with its orientation shown as vectors pointing. Compare with figure 6 for the visualization of its weight and orientation.

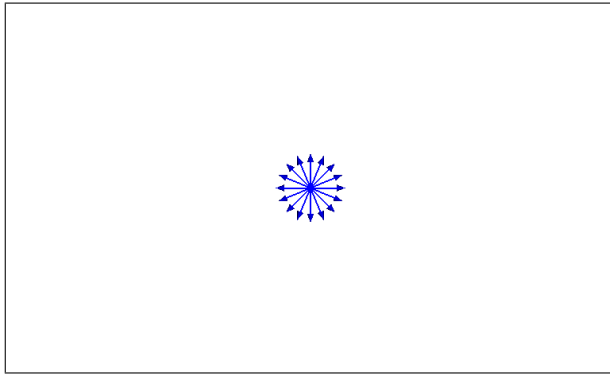


**Figure 9:** The pencil of lines  $(e_{01} + e_{02}) \wedge e_{12}$ . Compare with figure 22 for the visualization of its weight and orientation.

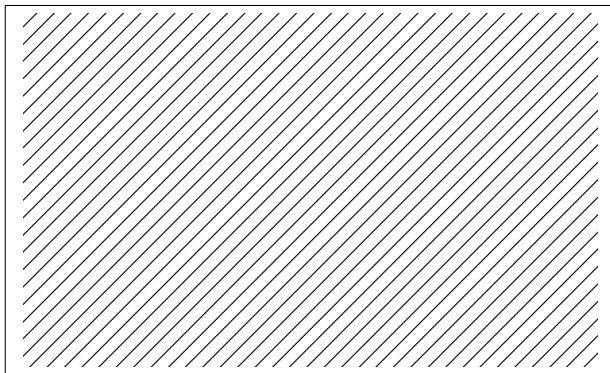


**Figure 10:** The pencil of ideal lines  $e_{23} \wedge e_{12}$  with its orientation shown.

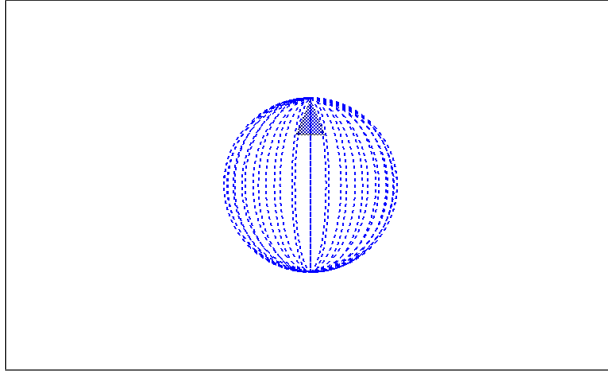


**Figure 11:** The hyperbolic linear line congruence  $e_{01} \wedge (e_{02} + e_{23})$ . Its orientation and weight are not shown.

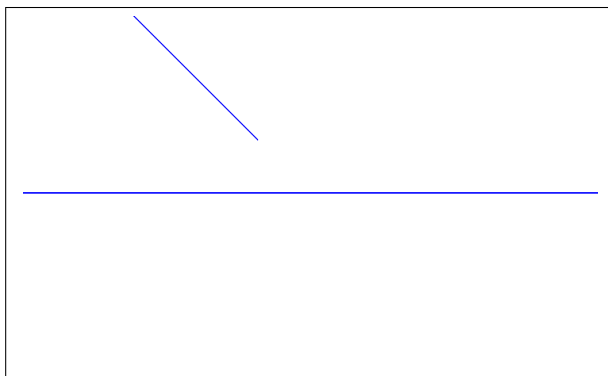


**Figure 12:** The hyperbolic linear line congruence  $-2e_{01} \wedge (e_{02} + e_{23})$  with its weight and orientation shown. Compare the length of the arrows with those of figure 2 for the visualization of the weight.

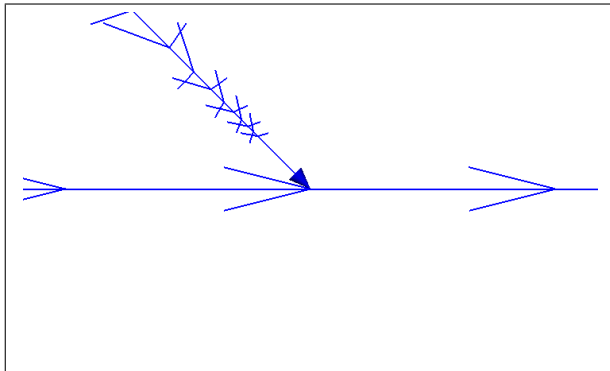


**Figure 13:** The hyperbolic linear line congruence  $2(e_{01} + e_{02}) \wedge (e_{23} + e_{12})$ . Compare with figure 12 for the visualization of its ideal line part. Compare with figure 3 for the visualization of the weight of its ideal line part.

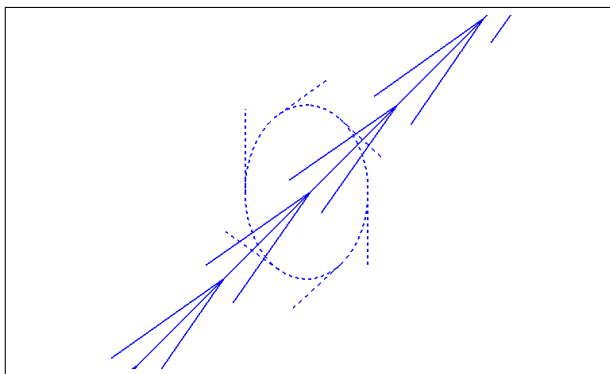


**Figure 14:** The hyperbolic pencil of linear complexes  $(e_{01} \wedge (e_{23} - e_{02}))^*$ . For a good insight of this figure, also consider figure 16. Compare with figure 15 for the visualization of the orientation.

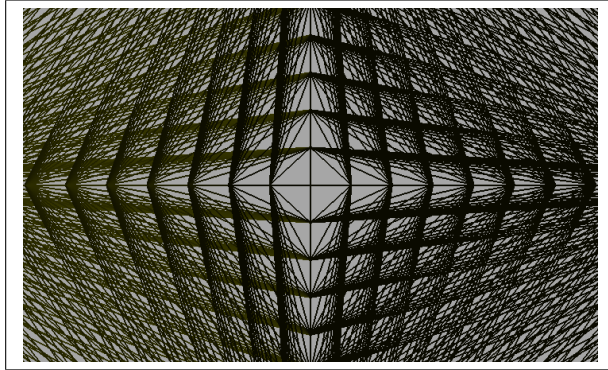


**Figure 15:** The hyperbolic pencil of linear complexes  $(e_{01} \wedge (e_{23} - e_{02}))^*$  with its orientation shown. Compare with figure 14 for the visualization of the orientation.

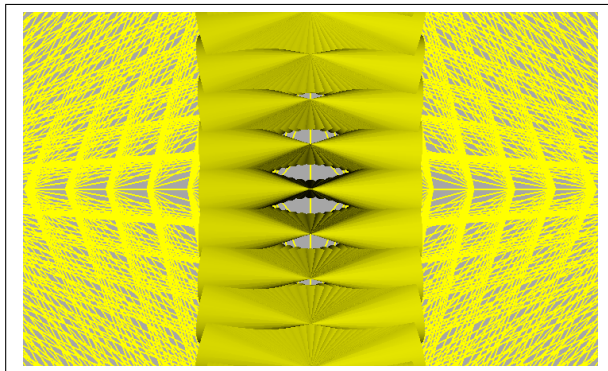


**Figure 16:** The hyperbolic pencil of linear complexes  $(e_{01} \wedge (e_{02} + e_{23}))^*$ . For a good insight of this figure, also consider figure 14.

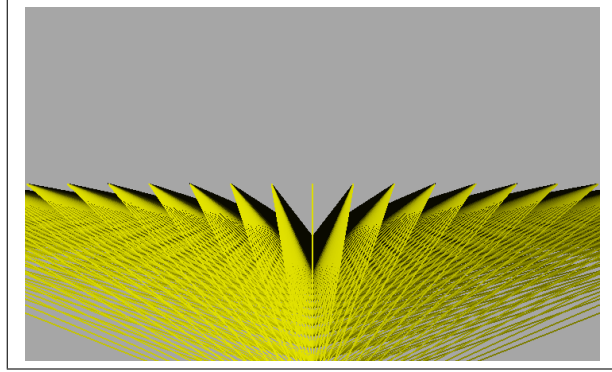


**Figure 17:** The hyperbolic pencil of linear complexes  $((e_{01} + e_{02}) \wedge (e_{23} + e_{12}))^*$ . Compare with figure 2 and figure 13 for the visualization of a line without weight and orientation. Compare with figure 13 for the color difference signifying grade, even though the drawing routines are the same.

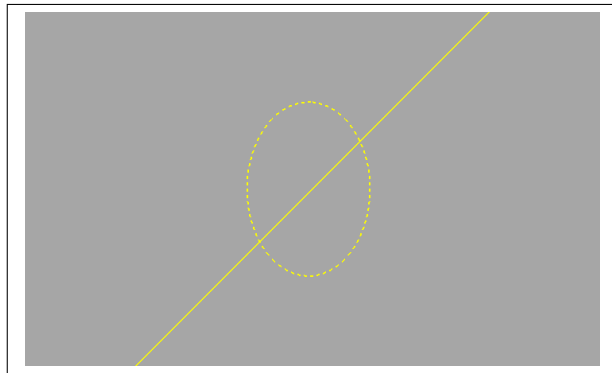


**Figure 18:** The points  $e_{01} \wedge (e_{02} - e_{12}) \wedge (e_{03} + e_{31})$  (left) and  $3e_{01} \wedge (e_{02} + e_{12}) \wedge (e_{03} - e_{31})$  (right). Compare the two points; their radius is the visual representation of their weight.

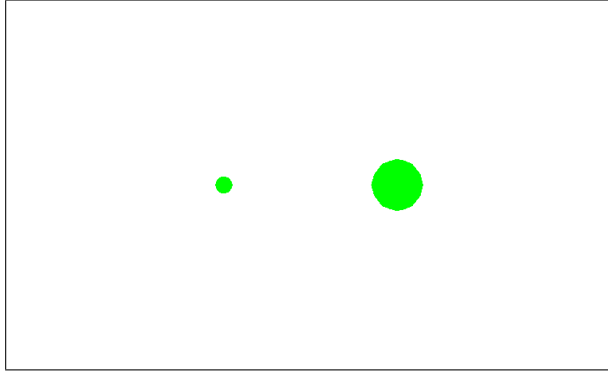


**Figure 19:** The ideal point  $3e_{01} \wedge e_{31} \wedge e_{12}$ . The distance between the two spheres is the visual representation of its weight. Compare with figure 20 for the visualization of its orientation.

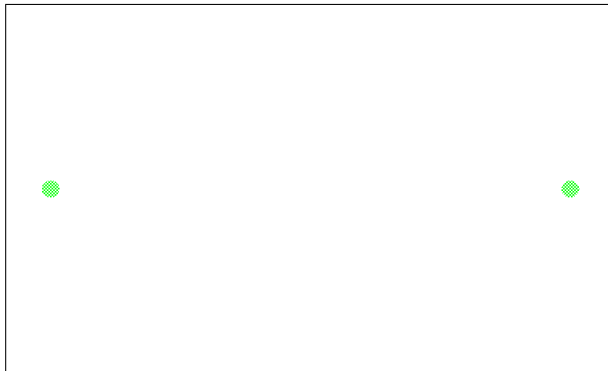


**Figure 20:** The ideal point  $e_{01} \wedge e_{31} \wedge e_{12}$ . The vector from one sphere to the other is the visual representation of its orientation. Compare with figure 20 for the visualization of its weight.

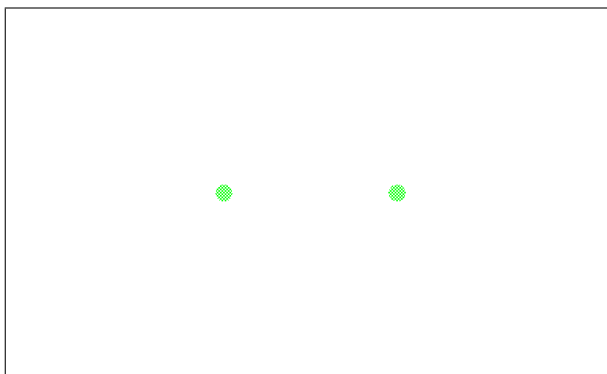


**Figure 21:** The plane  $e_{01} \wedge e_{03} \wedge (e_{01} - e_{23} + 0.1e_{31} + e_{03} + e_{12})$ . Compare with figure 22 for the visualization of its orientation and weight.

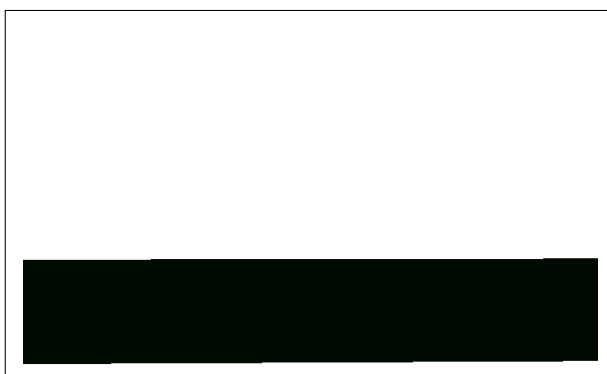


**Figure 22:** The plane  $-e_{01} \wedge e_{03} \wedge (e_{01} - e_{23} + 0.1e_{31} + e_{03} + e_{12})$  with its weight and orientation visualized. The little green bars pointing up are the visualization of its weight and orientation.

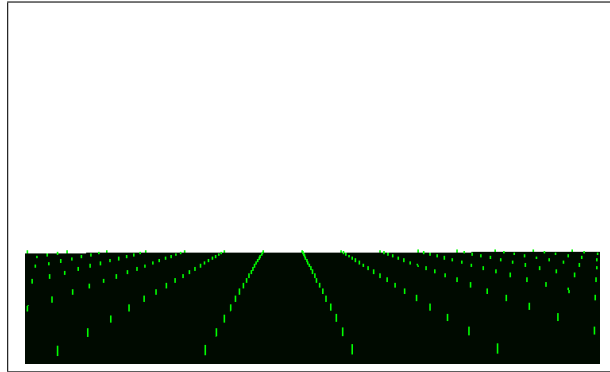


**Figure 23:** The ideal plane  $e_{23} \wedge e_{31} \wedge e_{12}$  with its weight and orientation visualized. Compare the radius of the sphere with figure 24 for the visualization of the weight.

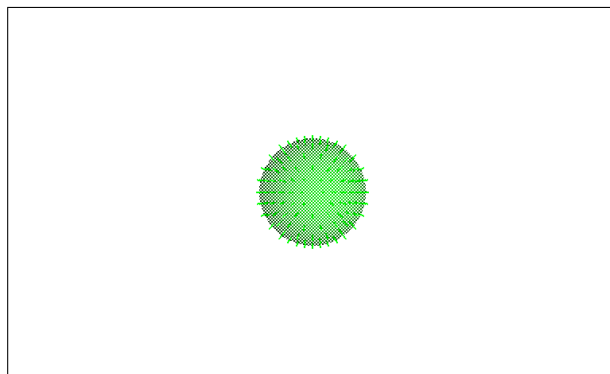




**Figure 24:** The ideal plane  $-4e_{23} \wedge e_{31} \wedge e_{12}$  with its weight and orientation visualized. The direction of the green bars indicate the plane's orientation. Compare the radius of the sphere with figure 23 for the visualization of the weight.

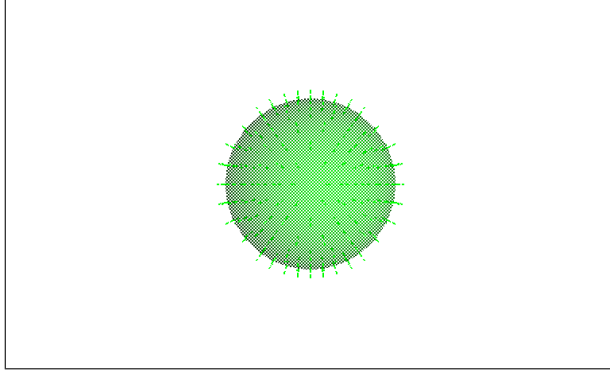
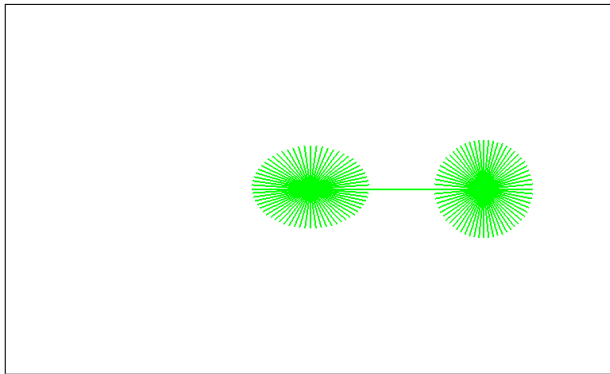


**Figure 25:** The couple-wheel pencil  $e_{01} \wedge (e_{02} + e_{03}) \wedge (e_{02} + 2e_{12})$ . Note that the pencils are connected with each other through the common line. The left pencil is tilted to the front.



## References

- [1] Johan Antony Barrau. *De ruimte*, volume 2 of *Analytische meetkunde*. Noordhoff, Groningen, 1918–1927.
- [2] Johan Antony Barrau. *Het platte vlak*, volume 1 of *Analytische meetkunde*. Noordhoff, Groningen, 1918–1927.
- [3] Leo Dorst. Projective transformations as versors. Working version of internal report (confidential; available on request from l.dorst@uva.nl), May 2012.
- [4] Leo Dorst, Daniel Fontijne, and Stephen Mann. *Geometric Algebra for Computer Science: An Object-Oriented Approach to Geometry (The Morgan Kaufmann Series in Computer Graphics)*. Morgan Kaufmann Publishers Inc., San Francisco, CA, USA, 2007.
- [5] Daniel Fontijne. *GAViewer Documentation: Version 0.84*. University of Amsterdam, March 2010. Code and binaries available at [http://geometricalgebra.org/gaviewer\\_download.html](http://geometricalgebra.org/gaviewer_download.html).
- [6] Daniel Fontijne, Tim Bouma, and Leo Dorst. *Gaigen: a Geometric Algebra Implementation Generator*. University of Amsterdam, July 2002. Code available at [http://www.science.uva.nl/ga/gaigen/files/20031124\\_gaigen.tar.gz](http://www.science.uva.nl/ga/gaigen/files/20031124_gaigen.tar.gz).
- [7] Hongbo Li and Lixian Zhang. Line geometry in terms of the null geometric algebra over  $\mathbb{R}^{3,3}$ , and application to the inverse singularity analysis of generalized stewart platforms. In Leo Dorst and Joan Lasenby, editors, *Guide to Geometric Algebra in Practice*, pages 253–272. Springer London, 2011.
- [8] Helmut Pottmann and Johannes Wallner. *Computational Line Geometry*, pages 133–158. Springer, August 2001.
- [9] K. Shoemake. Plucker coordinate tutorial. *Ray Tracing News*, 11(1), 1998.